Quantum-metric-enabled exciton condensate in double twisted bilayer graphene

Xiang Hu,[1] Timo Hyart,[2,3] Dmitry I. Pikulin,[4,5] and Enrico Rossi[1]

[1]*Department of Physics, William & Mary, Williamsburg, VA 23187, USA*
[2]*International Research Centre MagTop, Institute of Physics, Polish Academy of Sciences, Aleja Lotnikow 32/46, PL-02668 Warsaw, Poland*
[3]*Department of Applied Physics, Aalto University, 00076 Aalto, Espoo, Finland*
[4]*Microsoft Quantum, Redmond, Washington 98052, USA*
[5]*Microsoft Quantum, Station Q, Santa Barbara, California 93106-6105, USA*

(Dated: August 10, 2020)

Flat-band systems are a promising platform for realizing exotic collective ground states with spontaneously broken symmetry because the electron-electron interactions dominate the kinetic energy. A state of particular interest would be the chased after interlayer-phase-coherent exciton condensate but the conventional treatments of the effect of thermal and quantum fluctuations suggest that this state might be either unstable or fragile. In this work, using double twisted bilayer graphene heterostructures as an example, we show that the quantum metric of the Bloch wave functions can strongly stabilize the exciton condensate and reverse the conclusion that one would draw using a conventional approach. The quantum metric contribution arises from interband terms, and flat-bands are most commonly realized by engineering multiband systems. Our results therefore suggest that in many practical situations the quantum metric can play a critical role in determining the stability of exciton condensates in double layers formed by two-dimensional systems with flat-bands.

An exciton is a bosonic quasiparticle formed by an electron bound to a hole. In semiconductors excitons can be created by exciting electrons from the valence band to the conduction band with external photons: the electron-hole (e-h) pairs can then bind due to the Coulomb interaction. A large number of excitons can become phase coherent and form a collective state known as exciton condensate (EC) [1, 2]. Already in the mid 70's it was proposed [3, 4] that spatially separating electron and holes should facilitate the formation of a thermodynamically stable EC. Such separation can be realized in e-h semiconductor double layers, in which the two layers are separated by a thin dielectric that prevents interlayer tunneling but allows strong interlayer Coulomb interactions, and distinct metal gates for each layer are used to create an excess density of electrons in one layer which equals the excess density of holes in the other one, Fig. 1(a). The formation of an EC is expected to be further facilitated in double layers formed by systems with flat bands: the quenching of the kinetic energy increases the relative importance of the interaction terms and therefore should favor the realization of correlated ground states such as the EC. Indeed, some of the most compelling signatures of the presence of EC in double-layer systems have been observed in quantum Hall (QH) bilayers in which the kinetic term of each layer is completely quenched [5–10].

In recent years the great advances in the fabrication of heterostructures made possible the realization of several novel double layers in which ECs could be realized [11–30]. In particular, it was proposed that ECs could be formed in graphene double layers [11, 12], but experimentally no strong signatures have been observed. It was then proposed that ECs could be realized in systems based on double bilayer graphene [14, 15, 22] and recent experiments have shown that two graphene bilayers separated by an insulating barrier indeed show signatures that are consistent with the formation of EC [24]. Considering that at low energies the bands of bilayer graphene are quadratic whereas the bands of graphene are linear, these recent findings suggest that the higher density of states is important in the formation of EC. Extrapolating this reasoning, combined with the results for QH bilayers, would suggest that in general bilayers formed by 2D systems with reasonably flat bands should support the formation of ECs. As a consequence, twisted bilayer graphene (TBLG), in which the bands can be made extremely flat by tuning the twist angle θ between graphene sheets [31–37] appears to be the ideal 2D system to seek the realization of robust ECs without external magnetic fields. This expectation, however, is in part naïve for two reasons: (i) The flatness of the bands is associated to a large density of states and therefore a strong screening (reduction) of the interlayer Coulomb interaction that is the driver of the EC instability; (ii) The stiffness of the EC, i.e. its stability against thermal and quantum fluctuations, is conventionally expected to decrease as the bands become flatter and ultimately vanish in the limit of perfectly flat bands. Here, the lack of the particle-hole symmetry of the valence and conduction bands also contributes to the fragility of the EC. The first obstacle can be overcome by tuning the system into the strong coupling regime, where the electron and hole densities are sufficiently small so that the coherence length ξ of the EC is smaller than the average distance between particles [16].

In this work we show that the second obstacle in general might not be present if one considers the contribution to the EC's stiffness due to the quantum metric of the eigenstates of the EC. Such contribution is due to interband terms in the expression for ρ_s and therefore must be always carefully accounted for in multiband systems. We consider the specific case of double layers formed by an electron-doped TBLG and a hole-doped TBLG separated by a thin insulating barrier, Fig. 1 (a), and show that for these systems the quantum metric contribution to ρ_s strongly stabilizes the EC. In addition, we obtain how ρ_s depends on the twist angle and find that the

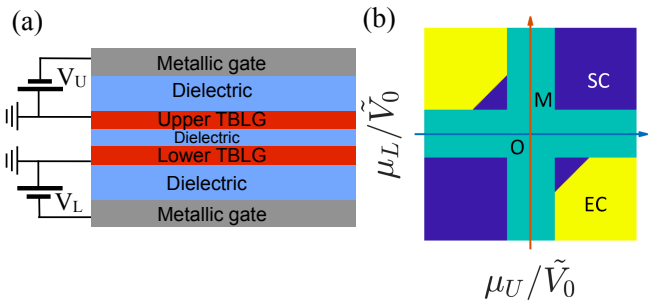

FIG. 1. (a) Sketch of a double TBLG system. (b) Phase diagram of a double layer system with ideal flat bands calculated based on the the symmetry-broken state with the largest critical temperature. At low dopings a correlated insulating state has the largest critical temperature (light blue region). At higher layer-symmetric doping $\mu_L \approx \mu_U$ superconductivity prevails (dark blue regions). In the case of sufficiently large *layer-antisymmetric* doping $\mu_L \approx -\mu_U$ the interlayer phase coherent EC is favored (yellow region). Here $\tilde{V}_0$ is the effective interaction strength for the correlated insulator states.

most favorable twist angle θ to realize a stable EC is not the magic angle. Using these results we obtain the Berezinskii-Kosterlitz-Thouless (BKT) temperature $T_{\rm BKT}$ as function of θ. Considering that most systems with almost flat bands are multiband systems, our results have universal relevance for the understanding of the conditions necessary to realize ECs: they show that to realize an EC in 2D bilayers at relatively high temperature the flatness of the bands of the layers must be accompanied by a significant quantum metric contribution to the EC's stiffness. Our results also allow to understand in a new light the conditions that make possible the realization and observation of ECs in QH bilayer [38, 39].

The double TBLG system is described by the Hamiltonian $\hat{H} = \hat{H}^U + \hat{H}^L + \hat{H}_{int}$ where $\hat{H}^{U/L}$ is the Hamiltonian describing the upper/lower TBLG and H_{int} describes the interaction between electrons in the upper (U) and lower (L) TBLG. We assume θ to be the same for the two TBLGs. For small twist angles the low energy states of a TBLG are well described [33] by an effective tight-binding (TB) Hamiltonian in momentum space for a triangular lattice. The lattice sites are identified by the reciprocal lattice wave vectors $\{\mathbf{b} = m_1\mathbf{b}_1 + m_2\mathbf{b}_2\}$ of the moiré lattice formed by the twisted graphene sheets, where $\mathbf{b}_1 = (\sqrt{3}Q, 0), \mathbf{b}_2 = (\sqrt{3}Q/2, 3Q/2)$, $Q = (8\pi/3a_0)\sin(\theta/2)$ and a_0 is the lattice constant of graphene. The onsite block at each momentum space lattice site $\mathbf{b}$, corresponding to the $\mathbf{K}$ valley of the graphene sheets, is described by Hamiltonian

$$H^{(t/b)}_{\mathbf{Kb}}(\mathbf{k}) = e^{\mp i\frac{\theta}{4}\sigma_z}[\hbar v_F(\mathbf{k} - \boldsymbol{\kappa}_{\mathbf{b}\pm})\cdot\boldsymbol{\sigma} - \mu\sigma_0]e^{\pm i\frac{\theta}{4}\sigma_z}, \quad (1)$$

where the first (second) sign is associated to the t (b) graphene sheet, σ_i are Pauli matrices in sublattice A/B space, $v_F = 10^6$ m/s is Fermi velocity in graphene, $\mathbf{k}$ is the electron wave vector (measured from $\mathbf{K}$), $\boldsymbol{\kappa}_{\mathbf{b}\pm} = \mathbf{b} + \boldsymbol{\beta}_\pm$, $\boldsymbol{\beta}_\pm = \{(0,0), (0,Q)\}$ are the momenta at the Dirac points of the two layers relative to each other, and μ is the chemical potential. The matrices $T_j = w[\tau_0 + \cos(2\pi j/3)\tau_x + \sin(2\pi j/3)\tau_y]$ with $j = -1, 0, 1$ describe the hopping from b to t layer corresponding to shift in the momentum space lattice by $\mathbf{b}_2 - \mathbf{b}_1$, $\mathbf{0}$ and $\mathbf{b}_2$, respectively [33]. $H_{\mathbf{K}'}$ is obtained from $H_{\mathbf{K}}$ via time reversal operation. Here $w = 118$ meV [40, 41].

In double TBLG the interactions have an intralayer and an interlayer component. Let $\mu_{U/L}$ be the chemical potential in the upper/lower TBLG. When $\mu_U \sim \mu_L$ the intralayer component of the interaction dominates and at low temperature correlated ground states are realized in each TBLG [34–37], see Fig. 1(b). Close to half-filling $\mu_L, \mu_U \to 0$ one realizes correlated insulating phases and by doping away from the half-filling superconducting phase is realized. However, when $\mu_U \sim -\mu_L$ the excess density of electrons in one of the layers approximately equals the excess density of holes in the other layer and the EC state is expected to be favored [Fig. 1(b)]. Therefore, in the remainder we set $\mu_L = -\mu_U \equiv \mu$ and neglect the effect of the intralayer interactions which only renormalize the parameters of the model. For simplicity we assume that the interlayer interaction is local $\hat{H}_{int} = V_0\sum_{l\sigma l'\sigma'}\int d^2\mathbf{r} c^\dagger_{\mathbf{r}l\sigma U}c_{\mathbf{r}l\sigma U}c^\dagger_{\mathbf{r}l'\sigma' L}c_{\mathbf{r}l'\sigma' L}$ with effective interaction strength V_0 that can be obtained by integrating out the long-range Coulomb interaction, and $c^\dagger_{\mathbf{r}l\sigma T}$ ($c_{\mathbf{r}l\sigma T}$) the creation (annihilation) operator for an electron in the $T = U/L$ TBLG, at position $\mathbf{r}$, in graphene sheet $l = t/b$, and sublattice $\sigma = A/B$. We consider a spinless problem because we look for a solution obeying the spin-rotation symmetry. However, we point out that each layer has an independent spin-rotation symmetry, and therefore there exists a ground state degeneracy with respect to order parameters obtained via two independent spin rotations applied in the upper and lower TBLG, respectively. There exists also an approximate symmetry with respect to the rotations in the valley degree of freedom.

Focusing on the exchange part of H_{int}, we decouple it via the mean field and assume that the mean field obeys periodicity of the moiré superlattice, so that the exciton order parameter can be described via matrices $\Delta_{\mathbf{b}l\sigma l'\sigma'}$, which connect the lower TBLG to the upper TBLG and correspond to momentum shift $\mathbf{b}$ in the momentum space lattice. Close to the mean-field critical temperature T_c the Fourier components $\Delta_{\mathbf{b}l\sigma l'\sigma'}$ satisfy the linearized gap-equation $\Delta_{\mathbf{b}_1 l\sigma l'\sigma'} = \sum_{b_2 l_2\sigma_2 l'_2\sigma'_2}\chi^{\mathbf{b}_2 l_2\sigma_2 l'_2\sigma'_2}_{\mathbf{b}_1 l\sigma l'\sigma'}\Delta_{\mathbf{b}_2 l_2\sigma_2 l'_2\sigma'_2}$, with bare susceptibility

$$\chi^{\mathbf{b}_2 l_2\sigma_2 l'_2\sigma'_2}_{\mathbf{b}_1 l\sigma l'\sigma'} = \frac{V_0}{A}\sum_{\mathbf{b}\mathbf{b}'\mathbf{k}mn} U^{l\sigma}_{m,\mathbf{b}_1+\mathbf{b}}(\mathbf{k})[U^{l'\sigma'}_{n,\mathbf{b}_1}(\mathbf{k})]^*$$
$$[U^{l_2\sigma_2}_{m,\mathbf{b}_2+\mathbf{b}'}(\mathbf{k})]^* U^{l'_2\sigma'_2}_{n,\mathbf{b}_2}(\mathbf{k})]\frac{n_F[\xi^L_n(\mathbf{k})]) - n_F[\xi^U_m(\mathbf{k})]}{\xi^U_m(\mathbf{k}) - \xi^L_n(\mathbf{k})}, \quad (2)$$

where A is the area of the sample, $\xi^{U(L)}_n(\mathbf{k})$ and $U^{l\sigma}_{n,\mathbf{b}}(\mathbf{k})$ are the eigenvalues and eigenstates of $\hat{H}^{U(L)}$, respectively. The critical temperature is obtained by finding the highest temperature for an eigenvalue of the bare susceptibility $\chi^{\mathbf{b}_2 l_2\sigma_2 l'_2\sigma'_2}_{\mathbf{b}_1 l\sigma l'\sigma'}$ is equal to one. It is challenging to estimate the interaction

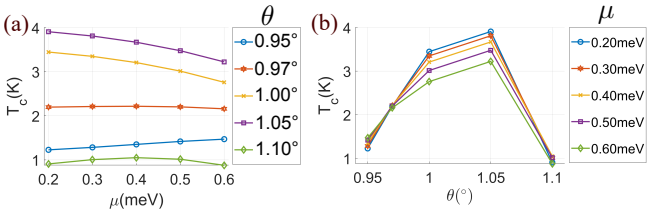

FIG. 2. (a) T_c as a function of $\mu = \mu_L = -\mu_U$ and different values of twist angle θ. (b) T_c as a function of θ and different values of μ.

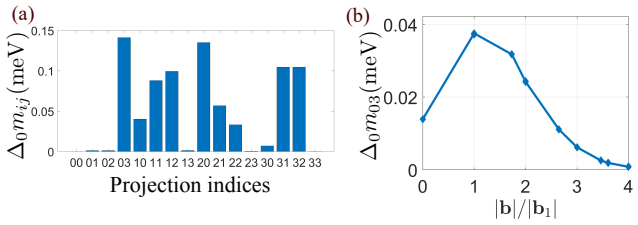

FIG. 3. (a) Amplitudes of the order parameter components $\Delta_0 m_{ij}$ in the layer i and sublattice j space. (b) Scaling with $|\mathbf{b}|$ of the largest projection of the EC's order parametes with $\Delta_{03} = \Delta_0 m_{03}$. For both plots, the twist angle $\theta = 1.05^\circ$ and $\mu = 0.30$meV.

strength V_0 because of the the interplay of screening effects and collective instabilities, but since the focus of our work is the stability of the EC arising from the quantum metric we adopt the pragmatic approach and fix it so that the critical $T_c \sim 4$ K around the magic angle is of the same order as measured experimentally for the correlated states of isolated TBLGs [34–37]. We use $V_0 = 100$ meV$\cdot$ nm^2 which satisfies this requirement along with putting the system into the strong-coupling regime. Below the critical temperature we assume that the amplitude of the mean field obeys $\Delta_0 \equiv \| \sum_{\mathbf{b},l,l',\sigma,\sigma'} \Delta_{\mathbf{b}_1}(l\sigma l'\sigma') \| = 1.764 k_B T_c (1 - T/T_c)^{1/2}$, where k_B is the Boltzmann's constant.

Figure 2 (a) shows how T_c scales with $\mu = \mu_L = -\mu_U$ for different values of θ close to $\theta_M = 1.05^\circ$. All the results of Fig. 2, and in the remainder, have been obtained keeping all the $\mathbf{b}$ for which $|\mathbf{b}| \leq 4|\mathbf{b}_1|$, but including larger momentum shifts does not change our results significantly. We see that T_c depends fairly weakly on μ, especially away from θ_M. Figure 2 (b) shows the evolution of T_c with θ for different values of μ around half-filling. For all the values of μ considered T_c is always largest at the magic angle, a consequence of the fact that the bands are flattest, and therefore the density of states larger, at this angle. The results of Fig. 2 also show that T_c decreases reasonably quickly when tuning θ away from θ_M.

The solution of the linearized gap equation reveals that the EC's order parameter, $\Delta_{\mathbf{b}l\sigma l'\sigma'}$, has several non-zero components. To better understand the orbital structure of $\Delta_{\mathbf{b}l\sigma l'\sigma'}$ we calculate its projections m_{ij} in the $\kappa_i \otimes \sigma_j$ space, where κ_i are the Pauli matrices in the layer index t, b. We have $m_{ij} = [\sum_{\mathbf{b}} (a_{ij}^{(\mathbf{b})})^2]^{1/2}$ and $a_{ij}^{(\mathbf{b})} = (1/4)\mathrm{Tr}[\Delta_{\mathbf{b}}(l\sigma l'\sigma')\kappa_i \otimes \sigma_j]$. The values of m_{ij} are shown in Fig. 3 (a). By analogy to the case of simple double-layer graphene [11, 12] and double bilayer graphene [14, 15, 22] we would expect certain specific components of m_{ij} to be dominant. From Fig. 3 (a) we see that m_{03} is the largest projection, however it is not dominant: several other projections have similar amplitude, in particular m_{20}, m_{31} and m_{32} are comparable to m_{03}. The fairly even distribution of the EC's order parameter over different orbital channels is paralleled by its fairly slow decay with the magnitude of the reciprocal lattice wave-vectors $\mathbf{b}$ [Fig. 3 (b)]. This is in contrast with the results for the case of superconducting pairing in isolated TBLG where the pairing is dominated by a single channel and the magnitude of the order parameter decreases quickly as a function of increasing $|\mathbf{b}|$ [42, 43].

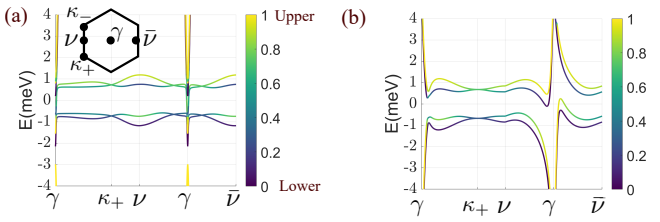

FIG. 4. Bandstructure in the exciton phase at zero temperature for $\theta = 1.05^\circ$ (a), and $\theta = 1.00^\circ$, (b). The colorbar indicates how much the eigenstate is localized in the upper or lower TBLG. The inset in (a) shows the moiré Brillouin zone.

Figure 4 shows the low energy bands along the $\gamma - \kappa_+ - \nu - \gamma - \bar{\nu}$ path in the moiré Brillouin zone (BZ) for $\theta = 1.05^\circ$, and $\theta = 1.00^\circ$ in the presence of the EC condensate. For $\theta = 1.05^\circ$ the very large Fermi velocity of the low energy bands at the γ point prevents the EC from opening a gap at this point. As θ is tuned away from θ_M the singularity at the γ point, Fig. 4 (a), morphs into two very small e-h pockets, Fig. 4 (b). The results of Fig. 4 show that in double layer TBLG the EC is expected to be, strictly speaking, gapless. However, given that the gapless nature is due to a very small number of states close to a single point of the BZ, the density of states is very negligible within the EC's gap, see, and so we expect that the transition to EC state could be clearly observed in the transport and spectroscopy measurements.

We now consider the stability of the EC with respect to fluctuations. The dominant fluctuations are the ones of the phase, $\varphi(\mathbf{r})$, of the order parameter: $\Delta \to \Delta e^{i\varphi(\mathbf{r})}$. Expanding the action in the long-wavelength limit around the saddle point identified by the mean-field solution we have $S = \hat{S}_0 + \int d\tau \int d\mathbf{r} \frac{1}{2} \rho^s_{\alpha\beta} \partial_{r_\alpha} \varphi \partial_{r_\beta} \varphi$, where S_0 is the action at the saddle point, and $\rho^s_{\alpha\beta}$ is the $\alpha\beta$ component of the EC's stiffness. The EC is stable when ρ^s is positive-definite. For a multiband system ρ^s is given by the general expres-

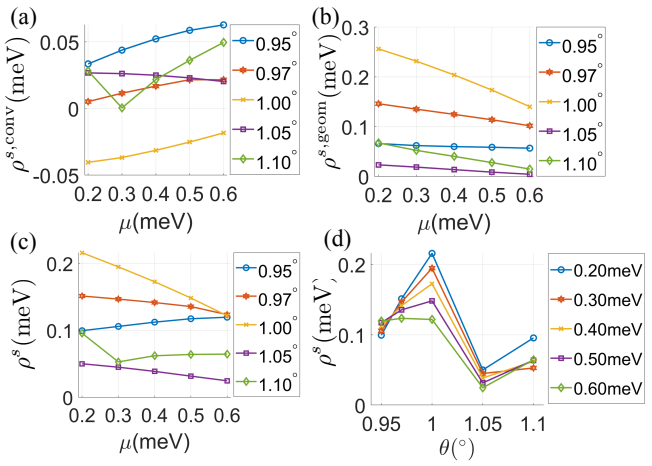

FIG. 5. Conventional $\rho^{s,\mathrm{conv}}$ (a), geometric $\rho^{s,\mathrm{geom}}$ (b), and total stiffness ρ^s (c), as a function of μ for different values of θ. (d) ρ^s vs. θ for different values of μ.

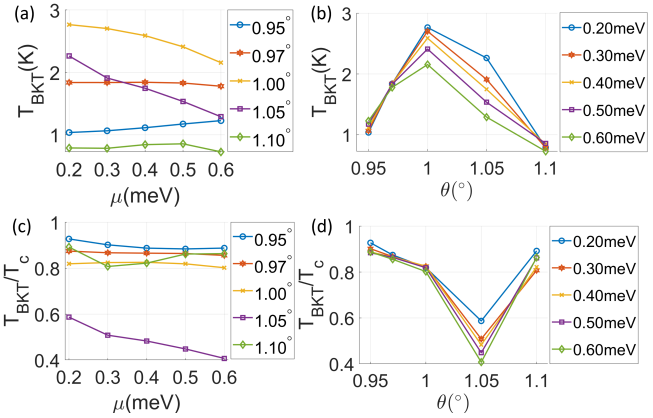

FIG. 6. (a) T_{BKT} as a function of μ for different values of θ. (b) T_{BKT} as a function of θ for different values of μ. (c), (d) T_{BKT}/T_c as a function of μ, θ, respectively.

sion [44, 45]:

$$\rho^s_{\alpha\beta} = \sum_{\mathbf{k},i,j} \frac{n_F(E_j) - n_F(E_i)}{E_i - E_j} \left(\frac{1}{4A} \langle\psi_i|\hat{v}_\alpha|\psi_j\rangle\langle\psi_j|\hat{v}_\beta|\psi_i\rangle - \frac{1}{A}\langle\psi_i|\hat{v}_{cf,\alpha}|\psi_j\rangle\langle\psi_j|\hat{v}_{cf,\beta}|\psi_i\rangle \right), \tag{3}$$

where E_i, $|\psi_i\rangle$, are the eigenvalues, eigenstates, of the mean-field Hamiltonian, H_{MF}, $\hat{v}_\alpha(\mathbf{k}) = \partial H_{\mathrm{MF}}/\partial k_\alpha$, $\hat{v}_{cf,\alpha}(\mathbf{k}) = (1/2)\gamma_z \partial H_{\mathrm{MF}}/\partial k_\alpha$, are the α components of the regular and counterflow velocity operators, respectively (γ_z is the Pauli matrix acting in the U/L subspace). In our case $\mathbf{k} = (k_x, k_y)$, $\rho^s_{xy} = \rho^s_{yx} = 0$, and $\rho^s_{xx} = \rho^s_{yy} \equiv \rho_s$. From Eq. (3) we have that for a multi-band system both intraband and interband terms contribute to ρ_s. We can therefore separate these contributions $\rho^s = \rho^{s,\mathrm{conv}} + \rho^{s,\mathrm{geom}}$ where $\rho^{s,\mathrm{conv}}$ is the conventional contribution arising almost exclusively from intraband terms, and $\rho^{s,\mathrm{geom}}$ is the contribution arising only from interband terms. $\rho^{s,\mathrm{geom}}$ is closely connected to the quantum metric of the Hilbert space spanned by the eigenstates of H_{MF} [43–48], hence the name.

Figure 5 (a), (b), (c) show how $\rho^{s,\mathrm{conv}}$, $\rho^{s,\mathrm{geom}}$ and ρ^s, respectively, vary with μ for different values of θ. Figure 5 (d) shows the evolution of ρ^s with θ for different values of μ. All the results where obtained for a temperature equal to 20 mK, much smaller than all values of T_c. Figure 5 is the main result of this work. We notice that ρ_s does not grow with μ contrary to the conventional result $\rho_s \propto \mu$. For $\theta = 1.05°$, and $\theta = 1.10°$, $\rho^{s,\mathrm{conv}}$ and $\rho^{s,\mathrm{geom}}$ are comparable and the relative weight changes with μ [49]. For all the other twist angles considered $\rho^{s,\mathrm{geom}}$ is larger than $\rho^{s,\mathrm{conv}}$, regardless of μ.

The results of Fig. 2 (a) show that for $\theta = 1.00°$ the mean field T_c was slightly smaller than the value of T_c at the magic angle, making double-layer TBLG with $\theta = 1.00°$ one of the best candidates for the realization of an EC. Strikingly, for $\theta = 1.00°$, we find that $\rho^{s,\mathrm{conv}}$ is negative, for all the values of μ, Fig. 5 (a). This can happen because of the lack of particle-hole symmetry between the electron and hole bands. This result would lead us to conclude that for $\theta = 1.00°$ the EC is fragile against fluctuations and therefore not a stable ground state, despite the relatively large value of T_c. This conclusion is reversed if one takes into account the geometric contribution to ρ_s, Fig. 5 (b): for $\theta = 1.00°$ the $\rho^{s,\mathrm{geom}}$ is positive and much larger, in absolute value, than $\rho^{s,\mathrm{conv}}$, guaranteeing the robust stability of the EC. Figures 5 (c), (d) allow us to identify for which value of θ and μ the EC is most stable. We see that for all the values of μ the EC is most stable for $\theta = 1.00°$, not for θ equal to the magic angle, as suggested by the mean-field results.

The results of Fig. 5 (c), (d), can be used to obtain the critical temperature, T_{BKT}, for the BKT phase transition [50, 51] via the equation $k_B T_{\mathrm{BKT}} = 2\pi\rho^s[\Delta[T_{\mathrm{BKT}}], T_{\mathrm{BKT}}]$, where we have taken into account the valley and spin degeneracies. Using this relation we can obtain the full temperature dependence of ρ_s, and then T_{BKT}. The results are shown in Fig. 6. From Fig. 6 (a), (b) we see that, contrary to the mean-field results, the twist angle for which the critical temperature T_{BKT} is largest is not θ_M, but $\theta = 1.00°$, for all the values of μ. Indeed T_{BKT} at $\theta = 1.00°$ is up to 50% larger than at θ_M. This is a somewhat surprising results that is entirely due to the geometric contribution to ρ_s. It is interesting to notice that, contrary to the conventional wisdom, for some twist angles T_{BKT} decreases, rather than increasing, with μ. Such behavior is particularly marked for $\theta = 1.00°$ and $\theta = \theta_M$ [Fig. 6 (a)] due to the significant decrease of the geometric contribution to stiffness as seen in Fig. 5. Figures 6 (c), (d) show how the ratio T_{BKT}/T_c scales with μ and θ, respectively. It is particularly interesting to see that, for all values of μ, T_{BKT}/T_c is minimum at θ_M. This result, combined with the result of Fig. 6 (b) lead us to conclude that the best candidate double-TBLG bilayer system to realize an EC is the one in which each

TBLG has $\theta = 1.00°$.

In summary, we showed that in flat-band double layers, such as double TBLG systems, the quantum metric plays a critical role for the realization of an interlayer-phase-coherent exciton condensate. We showed that, as expected, the flatness of the bands enhances the mean-field critical temperature T_c. However, the flatness of the bands, in general, also strongly suppresses the conventional part $\rho^{s,\mathrm{conv}}$ of the EC's stiffness. We found that indeed for double TBLG systems $\rho^{s,\mathrm{conv}}$ is very small and can even be negative due to the lack of particle-hole symmetry for configurations with high T_c. As a consequence the "conventional" study of the EC's stability that does not include interbands terms would lead to the conclusion that in flat-band double layers ECs can be unstable. However, we found that this conclusion is reversed if the interband terms responsible for the quantum metric of the flat-bands are taken into account: the quantum metric contribution to ρ^s can dominate over the conventional part and for the situations considered always guarantees the stability of the EC. We then used the temperature dependence of ρ^s to obtain T_{BKT} for the ECs in double TBLG systems and found that the largest T_{BKT} is realized not at the magic angle, $\theta = 1.05°$, but at $\theta = 1.00°$. Our results thus inform future experimental realizations of ECs in TBLG-based heterostructures. In a more general context, our findings point to the importance of the quantum metric for the understanding of the physics of ECs in flat band systems, including QH bilayers. For the long-standing effort to realize ECs without magnetic fields our findings show that the focus should not be on single-band systems in which the flat bands are obtained by tuning the hopping parameters, but on multi-band systems in which the low-energy flat bands can be engineered to lead to a large geometric contribution to the superfluid stiffness due to the quantum metric of the Bloch wave functions.

X.H and E.R. acknowledge support from ARO (Grant No. W911NF-18-1-0290) and NSF (Grant No. DMR- 1455233). E.R. also thanks the Aspen Center for Physics, which is supported by NSF Grant No. PHY-1607611, and KITP, supported by Grant No. NSF PHY1748958, where part of this work was performed. The authors acknowledge William & Mary Research Computing for providing computational resources that have contributed to the results reported within this paper. The research was partially supported by the Foundation for Polish Science through the IRA Programme co-financed by EU within SG OP.

[1] L. V. Keldysh and Yu. E. Kopaev, "Possible instability of the semimetallic state toward Coulomb interaction," Sov. Phys. Solid State **6**, 2219 (1965).

[2] B.I. Halperin and T.M. Rice, "The excitonic state at the semiconductor-semimetal transition," (Academic Press, 1968) pp. 115 – 192.

[3] Y E Lozovik and V I Yudson, "Feasibility of superfluidity of paired spatially separated electrons and holes - new superconductivity mechanism," Jetp Lett. **22**, 274 (1975).

[4] Y. E. Lozovik and V. I. Yudson, "Novel mechanism of superconductivity - pairing of spatially separated electrons and holes," Zhurnal Eksperimentalnoi I Teoreticheskoi Fiziki **71**, 738–753 (1976).

[5] I. B. Spielman, J. P. Eisenstein, L. N. Pfeiffer, and K. W. West, "Resonantly Enhanced Tunneling in a Double Layer Quantum Hall Ferromagnet," Phys. Rev. Lett. **84**, 5808–5811 (2000).

[6] A. Stern, S. M. Girvin, A. H. MacDonald, and N. Ma, "Theory of interlayer tunneling in bilayer quantum Hall ferromagnets," Phys. Rev. Lett. **86**, 1829–1832 (2001).

[7] J. P. Eisenstein and A. H. MacDonald, "Bose-einstein condensation of excitons in bilayer electron systems," Nature **432**, 691–694 (2004).

[8] Enrico Rossi, Alvaro S. Núñez, and A. H. MacDonald, "Interlayer Transport in Bilayer Quantum Hall Systems," Physical Review Letters **95**, 266804 (2005).

[9] A. D. K. Finck, J. P. Eisenstein, L. N. Pfeiffer, and K. W. West, "Exciton Transport and Andreev Reflection in a Bilayer Quantum Hall System," Physical Review Letters **106**, 236807 (2011).

[10] Timo Hyart and Bernd Rosenow, "Quantitative description of Josephson-like tunneling in $\nu_T = 1$ quantum Hall bilayers," Physical Review B **83**, 155315 (2011).

[11] Hongki Min, Rafi Bistritzer, Jung-Jung Su, and A. H. MacDonald, "Room-temperature superfluidity in graphene bilayers," Phys. Rev. B **78**, 121401 (2008).

[12] C.H. Zhang and Yogesh N. Joglekar, "Excitonic condensation of massless fermions in graphene bilayers," Phys. Rev. B **77**, 233405 (2008).

[13] Maxim Yu. Kharitonov and Konstantin B. Efetov, "Electron screening and excitonic condensation in double-layer graphene systems," Physical Review B **78**, 241401 (2008).

[14] Junhua Zhang and E. Rossi, "Chiral superfluid states in hybrid graphene heterostructures," Phys. Rev. Lett. **111**, 086804 (2013).

[15] A. Perali, D. Neilson, and A. R. Hamilton, "High-temperature superfluidity in double-bilayer graphene," Phys. Rev. Lett. **110**, 146803 (2013).

[16] D. Neilson, A. Perali, and A. R. Hamilton, "Excitonic superfluidity and screening in electron-hole bilayer systems," Phys. Rev. B **89**, 060502 (2014).

[17] D. I. Pikulin and T. Hyart, "Interplay of exciton condensation and the quantum spin hall effect in $\mathrm{InAs/GaSb}$ bilayers," Phys. Rev. Lett. **112**, 176403 (2014).

[18] M. M. Fogler, L. V. Butov, and K. S. Novoselov, "High-temperature superfluidity with indirect excitons in van der Waals heterostructures," Nature Communications **5**, 4555 (2014).

[19] D. I. Pikulin, P. G. Silvestrov, and T. Hyart, "Confinement-deconfinement transition due to spontaneous symmetry breaking in quantum Hall bilayers," Nature Communications **7**, 10462 (2016).

[20] J. I. A. Li, T. Taniguchi, K. Watanabe, J. Hone, and C. R. Dean, "Excitonic superfluid phase in double bilayer graphene," Nature Physics **13**, 751–755 (2017).

[21] Bishwajit Debnath, Yafis Barlas, Darshana Wickramaratne, Mahesh R. Neupane, and Roger K. Lake, "Exciton condensate in bilayer transition metal dichalcogenides: Strong coupling regime," Physical Review B **96**, 174504 (2017).

[22] Jung-Jung Su and Allan H. MacDonald, "Spatially indirect exciton condensate phases in double bilayer graphene," Phys. Rev. B **95**, 045416 (2017).

[23] Lingjie Du, Xinwei Li, Wenkai Lou, Gerard Sullivan, Kai Chang, Junichiro Kono, and Rui-Rui Du, "Evidence for a topo-

logical excitonic insulator in InAs/GaSb bilayers," Nature Communications **8**, 1971 (2017).

[24] G. William Burg, Nitin Prasad, Kyounghwan Kim, Takashi Taniguchi, Kenji Watanabe, Allan H. MacDonald, Leonard F. Register, and Emanuel Tutuc, "Strongly enhanced tunneling at total charge neutrality in double-bilayer graphene-WSe_2 heterostructures," Phys. Rev. Lett. **120**, 177702 (2018).

[25] Kha Tran, Galan Moody, Fengcheng Wu, Xiaobo Lu, Junho Choi, Kyounghwan Kim, Amritesh Rai, Daniel A Sanchez, Jiamin Quan, Akshay Singh, *et al.*, "Evidence for moiré excitons in van der Waals heterostructures," Nature **567**, 71–75 (2019).

[26] Zefang Wang, Daniel A. Rhodes, Kenji Watanabe, Takashi Taniguchi, James C. Hone, Jie Shan, and Kin Fai Mak, "Evidence of high-temperature exciton condensation in two-dimensional atomic double layers," Nature **574**, 76–80 (2019).

[27] Xiaomeng Liu, Zeyu Hao, Kenji Watanabe, Takashi Taniguchi, Bertrand I. Halperin, and Philip Kim, "Interlayer fractional quantum Hall effect in a coupled graphene double layer," Nature Physics **15**, 893–897 (2019).

[28] Yves H. Kwan, Yichen Hu, Steven H. Simon, and S. A. Parameswaran, "Excitonic fractional quantum Hall hierarchy in moiré heterostructures," arXiv:2003.11559 (2020).

[29] Yves H. Kwan, Yichen Hu, Steven H. Simon, and S. A. Parameswaran, "Exciton band topology in spontaneous quantum anomalous Hall insulators: applications to twisted bilayer graphene," arXiv:2003.11560 (2020).

[30] Yuya Shimazaki, Ido Schwartz, Kenji Watanabe, Takashi Taniguchi, Martin Kroner, and Ataç Imamolu, "Strongly correlated electrons and hybrid excitons in a moiré heterostructure," Nature **580**, 1476 (2020).

[31] J. M. B. Lopes dos Santos, N. M. R. Peres, and A. H. Castro Neto, "Graphene bilayer with a twist: Electronic structure," Phys. Rev. Lett. **99**, 256802 (2007).

[32] E. Suárez Morell, J D Correa, P Vargas, M Pacheco, and Z Barticevic, "Flat bands in slightly twisted bilayer graphene: Tight-binding calculations," Physical Review B **82**, 121407 (2010).

[33] Rafi Bistritzer and A. H. MacDonald, "Moire bands in twisted double-layer graphene," Proceedings of the National Academy of Sciences **108**, 12233–12237 (2011).

[34] Yuan Cao, Valla Fatemi, Shiang Fang, Kenji Watanabe, Takashi Taniguchi, Efthimios Kaxiras, and Pablo Jarillo-Herrero, "Unconventional superconductivity in magic-angle graphene superlattices," Nature **556**, 43 (2018).

[35] Yuan Cao, Valla Fatemi, Ahmet Demir, Shiang Fang, Spencer L. Tomarken, Jason Y. Luo, Javier D. Sanchez-Yamagishi, Kenji Watanabe, Takashi Taniguchi, Efthimios Kaxiras, Ray C. Ashoori, and Pablo Jarillo-Herrero, "Correlated insulator behaviour at half-filling in magic-angle graphene superlattices," Nature **556**, 80 (2018).

[36] Matthew Yankowitz, Shaowen Chen, Hryhoriy Polshyn, Yuxuan Zhang, K. Watanabe, T. Taniguchi, David Graf, Andrea F. Young, and Cory R. Dean, "Tuning superconductivity in twisted bilayer graphene," Science **363**, 1059–1064 (2019).

[37] Xiaobo Lu, Petr Stepanov, Wei Yang, Ming Xie, Mohammed Ali Aamir, Ipsita Das, Carles Urgell, Kenji Watanabe, Takashi Taniguchi, Guangyu Zhang, Adrian Bachtold, Allan H. MacDonald, and Dmitri K. Efetov, "Superconductors, orbital magnets and correlated states in magic-angle bilayer graphene," Nature **574**, 653–657 (2019).

[38] K. Yang, K. Moon, L. Zheng, A. H. Macdonald, S. M. Girvin, D. Yoshioka, and S. C. Zhang, "Quantum ferromagnetism and phase-transitions in double-layer quantum Hall systems," Phys. Rev. Lett. **72**, 732 (1994).

[39] K. Moon, H. Mori, K. Yang, S. M. Girvin, A. H. Macdonald, L. Zheng, D. Yoshioka, and S. C. Zhang, "Spontaneous interlayer coherence in double-layer quantum Hall systems - charged vortices and Kosterlitz-Thouless phase-transitions," Phys. Rev. B **51**, 5138 (1995).

[40] Jeil Jung, Arnaud Raoux, Zhenhua Qiao, and A. H. MacDonald, "Ab initio theory of moiré superlattice bands in layered two-dimensional materials," Phys. Rev. B **89**, 205414 (2014).

[41] Stephen Carr, Shiang Fang, Pablo Jarillo-Herrero, and Efthimios Kaxiras, "Pressure dependence of the magic twist angle in graphene superlattices," Physical Review B **98**, 1–5 (2018).

[42] Fengcheng Wu, A. H. MacDonald, and Ivar Martin, "Theory of Phonon-Mediated Superconductivity in Twisted Bilayer Graphene," Physical Review Letters **121**, 257001 (2018).

[43] Xiang Hu, Timo Hyart, Dmitry I. Pikulin, and Enrico Rossi, "Geometric and conventional contribution to the superfluid weight in twisted bilayer graphene," Phys. Rev. Lett. **123**, 237002 (2019).

[44] Sebastiano Peotta and Päivi Törmä, "Superfluidity in topologically nontrivial flat bands," Nature Communications **6**, 8944 (2015).

[45] Long Liang, Tuomas I. Vanhala, Sebastiano Peotta, Topi Siro, Ari Harju, and Päivi Törmä, "Band geometry, Berry curvature, and superfluid weight," Phys. Rev. B **95**, 024515 (2017).

[46] Fang Xie, Zhida Song, Biao Lian, and B. Andrei Bernevig, "Topology-bounded superfluid weight in twisted bilayer graphene," Phys. Rev. Lett. **124**, 167002 (2020).

[47] A. Julku, T. J. Peltonen, L. Liang, T. T. Heikkilä, and P. Törmä, "Superfluid weight and Berezinskii-Kosterlitz-Thouless transition temperature of twisted bilayer graphene," Phys. Rev. B **101**, 060505 (2020).

[48] Jinlyu Cao, H. A. Fertig, and Luis Brey, "Quantum geometric exciton drift velocity," arXiv:2008.00259 [cond-mat.mes-hall].

[49] D. J. Scalapino, S. R. White, and S. C. Zhang, "Superfluid density and the Drude weight of the Hubbard model," Physical Review Letters **68**, 2830–2833 (1992).

[50] V. L. Berezinskiĭ, "Destruction of Long-range Order in One-dimensional and Two-dimensional Systems having a Continuous Symmetry Group I. Classical Systems," Soviet Journal of Experimental and Theoretical Physics **32**, 493 (1971).

[51] J M Kosterlitz and D J Thouless, "Ordering, metastability and phase transitions in two-dimensional systems," Journal of Physics C: Solid State Physics **6**, 1181–1203 (1973).